Agr. Nat. Resour. 56 (2022) 307–320

AGRICULTURE AND NATURAL RESOURCES

Journal homepage: http://anres.kasetsart.org

Research article

Monitoring of crop growth stages using Sentinel-1 synthetic aperture radar data

Anuphao Aobpaet

Department of Civil Engineering, Faculty of Engineering, Kasetsart University, Bangkok 10900, Thailand

Article Info

Article history:
Received 18 March 2021
Revised 10 February 2022
Accepted 11 February 2022
Available online 20 April 2022

Keywords:
Agricultural,
Crop,
Monitoring,
Sentinel-1 SAR,
Time Series

Abstract

Importance of the work: Given the ever-increasing scientific and practical interest in the implementation of satellite data from synthetic aperture radar (SAR) sensors in agriculture, it may be useful for successful crop monitoring to investigate the effects on the total backscatter signal of the biophysical characteristics of the vegetation, such as crop density, stem height and leaf arrangement.

Objectives: To monitor rice, maize, cassava and sugarcane for physical growth characteristics to develop an efficient production process based on capability evaluation of Sentinel-1 products using the mean change of backscatter of polarization, such as VV, VH, VV/VH and the radar vegetation index (RVI).

Materials & Methods: Sigma nought values were customized from the start of cultivation until harvest due to their sensitivity to soil moisture, leaf canopy and stem elongation. Time-series data were used from Sentinel-1 between January 2019 and August 2020. The level-1 ground range detection product resolutions were 20 m × 22 m (range by azimuth) with 10 m × 10 m pixel spacing. Sampling (100 points per crop) was used to establish the research area field boundary. Coverage was in Nakhon Ratchasima (15°N,102°E) and Khonkaen (16°N,102°E) provinces, Thailand.

Results: Statistical analysis using the t test identified the same crop growth stages of cassava, sugarcane and maize using VH polarization. The VV polarization was optimized for rice and cassava, while VV/VH was suitable for rice and maize. RVI could be applied to rice, maize and sugarcane. Finally, VV/VH for rice and VV/VH and RVI for maize could identify the different growth stages, while cassava and sugarcane had no identifiable polarization.

Main finding: The average sigma nought (in decibels) values of polarization from SAR sensors are appropriate to monitor and detect the physical growth of some economic crops in Thailand.

* Corresponding author.
E-mail address: fengaha@ku.ac.th (A. Aobpaet)

https://doi.org/10.34044/j.anres.2022.56.2.09

Introduction

There is a need to grow crops on suitable sites and obtain good yields considering their economic, social and environmental impacts making it necessary to focus on climate variability and adaptation to the specified conditions (Veloso et al., 2017). In general, remote sensing data using microwave systems can help monitor a crops' physical growth status with timely coverage of a large area and the ability to rerecord data for the same place for an exactly known recording time (time-series data analysis) is a beneficial technology for managing agricultural problems from local to global levels (Srikanth et al., 2021). Time-series data analysis can be used to identify when crops commence growing in each area, along with the day of harvest and other factors, such as the growing and mature states, harvest status, and where there has been no cultivation. This information will be helpful when working on crop planning. The Sentinel-1 SAR (synthetic aperture radar) is radar imaging that provides continuous images under all weather conditions, during the day or night. It offers high reliability due to the current good geographical coverage, quality of collected data and the rapid dissemination of data (The European Space Agency, 2020.). Baghdadi et al. (2011) mentioned that optical tracking of the crop's harvest status is highly potent and relies on interpretation by the human eye (Earth-i's Techniques, 2019). However, sometimes optical imagery is limited due to cloud cover and waiting for cloudless coverage may involve unacceptably long delays. This makes it challenging to keep track of crop growth status. On the other hand, SAR can overcome these limitations, helping monitor possible crop growth in any season.

The radar signal responds (sensitivity) to stimuli such as the roughness and wetness of the surface, which is an essential factor in monitoring the cultivation of crops, soil properties and planting planning; thus, it is helpful for land use assessment and harvest forecasting following the changes according to the planting season (The European Space Agency, 2020). Previous studies have shown that Sentinel-1 can monitor rice growing situations and improve planting plans. Due to the continuous real-time monitoring of the cultivated area with dual-polarization, VV and VH every 12 d, Aschbacher and Milagro-Pérez (2012) and Minh et al. (2019) explained that the polarization backscatter values are sensitive to water and the shape of vegetation. One study considered that time series analysis is the most popular data analysis method for identifying cultivated areas as single and dual-polarization can monitor and discriminate crop growth states (Schmitt and Brisco, 2013), and cross-polarization is associated with the growth of rice after cultivation. Due to the different polarization capacities (VV and VH), Mattia et al. (2003) found that rapeseed plantations in Italy and Sweden, there was an increase in the VH polarization rebound value as the leaf area index increased. Mattia et al. (2003) and Satalino et al. (2013) found that backscatters are susceptible to changes in crop structure and phylogenesis when wheat begins to germinate. Veloso et al. (2017) compared the Sentinel-1 time series with NDVI, finding that SAR and NDVI data were consistent, mainly regarding the VV/VH ratio used to track crop growth cycles. These studies demonstrate the potential of the Sentinel-1 SAR satellite to monitor crop changes.

The objective for the current study was to study the possibility of using a variety of Sentinel-1 polarization characteristics (VV, VH, VV/VH and RVI polarization patterns) to monitor the growth situations of significant crops in Thailand. Sentinel-1 is equipped with a SAR sensor in the C-band wavelength, and uses the interferometric wide (IW) swath in dual-polarization (VV+VH). The reflected wave power in decibels is plotted against the originally transmitted wave power. The logarithm equation results in a negative value denoted by the symbol σ^o (sigma nought). Because the reflected wave power is less than the transmitting wave's power, it is calculated in decibels (dB), as shown in Equation 1:

$$10 \log \left(\frac{P_2}{P_1}\right) = \text{dB} \quad (1)$$

Where P1 is the received energy by the sensor and P2 is the energy reflected in an isotropic way.

The mathematical equations from VV and VH polarization determine the vegetation covering the surface or the radar vegetation index (RVI).

Materials and Methods

Study area and crop growth stages

The study areas in this research were agricultural areas where the crops are mainly grown in the northeastern region of Thailand, in the Khon Kaen and Nakhon Ratchasima provinces (Fig. 1).

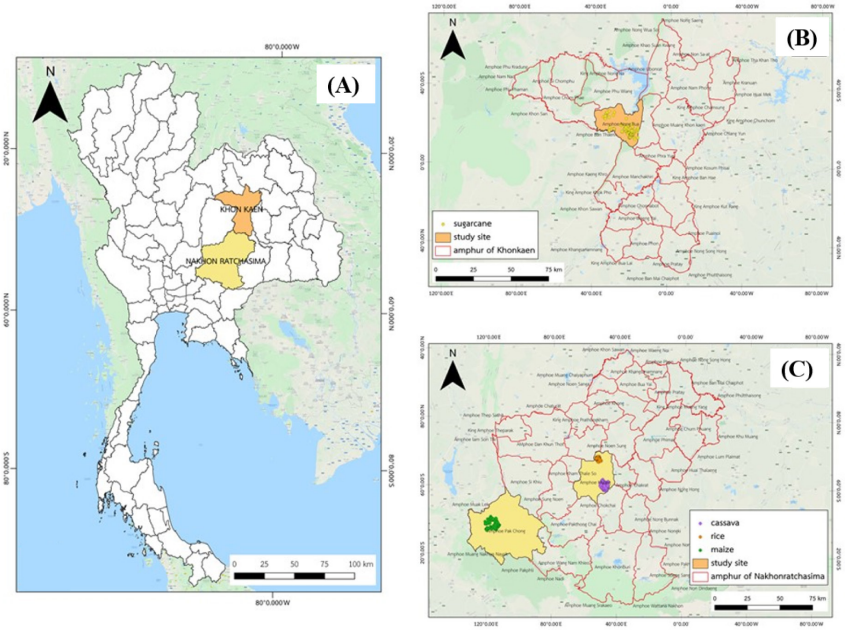

Fig. 1 (A) Nong Ruea district, Khon Kaen province; (B) Location of cassava and rice fields, Mueang district; (C) maize field location, Pak Chong district, Nakhon Ratchasima province

Khon Kaen province is located at 16°N and 102°E. It is an important province in northeast Thailand. The terrain is a flat, characterized by high and undulating slopes to the east and south. The province's major economic crops are rice, sugarcane, cassava and soybeans and Khon Kaen province is the third most important sugarcane cultivation area in northeast Thailand (Office of the Cane and Sugar Board, 2019).

Nakhon Ratchasima province is located on the Korat Plateau at 15°N and 102°E. The terrain contains both high mountains and lowland with undulating flat areas. The area produces the country's main crops—large factories in the agro-industrial sector support products, such as starch and ethanol factories from cassava, rice mill export, sugar processing and animal feed factories (Nakhon Ratchasima province, 2020).

Rice cultivation commences May–June and harvesting occurs November–January. The rice growth period is divided into three periods (Aguilar, 2019): 1) days 0–60, involving stem and leaf growth of the rice (beginning of germination to the highest tillering stage); 2) days 61–100 for reproductive development (inflorescence stage to flowering stage); 3) days 101–120 are the maturity period. Maize is planted May–July and harvested during December (Agromax Micronutrients Pvt. Ltd., 2018). The growth period of maize can be divided into two periods: stem and leaf growth and reproductive maturity. Stem and leaf maturation occur at age 0–60 d from germination to leaf and maize cob development. Maize can be harvested at age 120–160 d or more.

The growth period of cassava alternates between the storage of carbohydrates in the roots and the dormancy period. Planting commences at the beginning of the rainy season (May–June) and harvesting occurs in April–June of the following year. Organization for Economic Cooperation and Development (2016) divided cassava into five growth stages: budding; leaf development; root system formation; stem and leaf development; and carbohydrate relocation phase to the roots and dormancy. The initial sprouts emerge from internodes or buds underground at days 10–12. The development of true leaves begins to proliferate through photosynthesis approximately 30 days after planting. For shoots and roots, it begins where the roots grow in place of unnecessary roots. The newly formed roots penetrate the soil to a depth of 40–50 cm, absorbing water and nutrients, and 3–14 fuzzy roots become roots that store food. The next stage is the canopy development of cassava during days90–180. Branching extends from the ground cover during days 120–150 and then, the carbohydrate-to-root translocation phase commences during days 180–300. The nutrients are transferred from the leaves to the root; the leaves progressively wilt and fall until almost all of the leaves have abscised during days 300–360, when the dormancy period commences. Sugarcane has a growth period of approximately 360 d. The growth period of sugarcane is divided into four periods: sprouting; stem growth and blade (upper and interlaced) formation; peak growth; and maturity.

During days 0–60 is the erection period from the beginning of sugarcane germination until the shoot emerges out of the soil. During days 75–150, tillering depends on soil moisture, light, temperature and fertilizer during stem and leaf growth and the bud separates from the parent shoot. In the peak growth phase (days 150–240), sugarcane needs large amounts of water for stem extension to produce a high yield. Before harvesting, the maturity stage (days 240–360) involves slowing down of segment elongation and greater sugar accumulation in the stems.

Data used in research

Satellite image data

The analysis applied C-band SAR data from the Sentinel-1 satellite at Level-1 ground range detection with a pixel size of 10 m × 10 m. The frequency of the sensor is 5.405 GHz with an approximate 6 cm wavelength in interferometric wide (IW) swath mode. The IW swath mode is the primary acquisition mode over land and satisfies most service requirements. It acquires a 250 km swath of data at 5 m × 20 m spatial resolution (single look). Ascending satellites capture images every 12 d and all datasets used for processing must have the same properties, differing only in their orbiting resets in space. There are no weather restrictions impinging on the radar satellite data and it can be collected and downloaded free of charge via the ASF Data Search website (https://search.asf.alaska.edu/#/).

The current research used 35 images of Sentinel-1 SAR in path 99 and frames 1235 satellite covering an area in Khon Kaen province from 31 January 2019 to 5 August 2020 and path 99 and frame 1230, with 29 images covering an area in Nakhon Ratchasima province between 31 January 2019 and 17 August 2020.

Spatial data

The shapefile data were obtained from the website https://ecoplant.gistda.or.th/ and used to determine the field boundaries of the four main economic crops: rice, maize, cassava and sugarcane (Fig. 2). Then, the planting periods in each area were analyzed to estimate harvest days and the number of products available each time at each site.

Research methodology

The research work methods were divided into three main areas: 1) data preparation before analysis; 2) data analysis from satellite imagery; and 3) data analysis based on statistical analysis. Rainfall data was supplementary and was applied in the polarization analysis of the satellite imagery to describe rising polarization values and sudden drops during plant growth, depending for example on factors caused by rain in the study area or the water supply for plant growth. The process of analyzing all data can be summarized and displayed in the flowchart in Fig. 3.

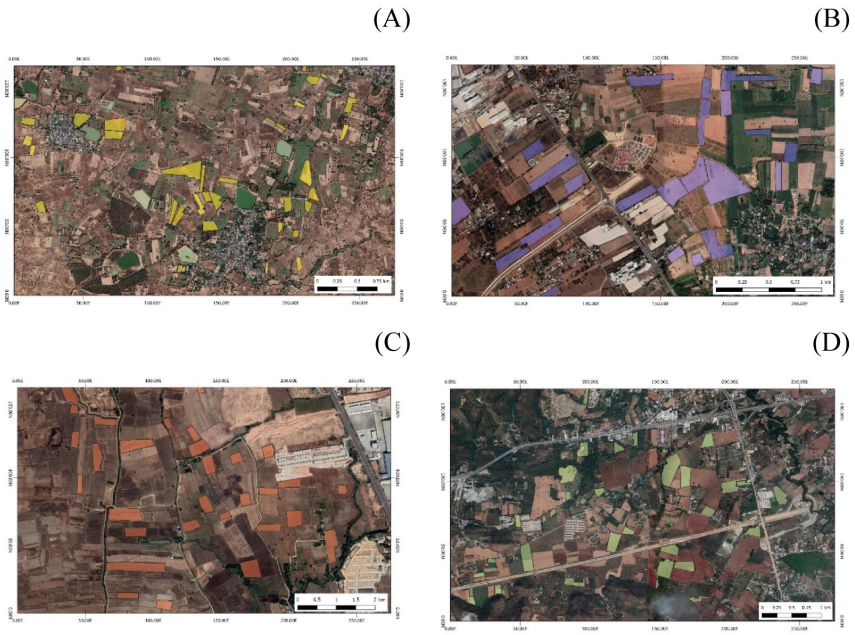

Fig. 2 (A) Sugarcane plots (yellow and green), Nong Ruea district, Khon Kaen province; (B) cassava plots (purple); (C) rice fields (brown), Mueang district, Nakhon Ratchasima province; (D) maize fields (green), Pak Chong district, Nakhon Ratchasima province

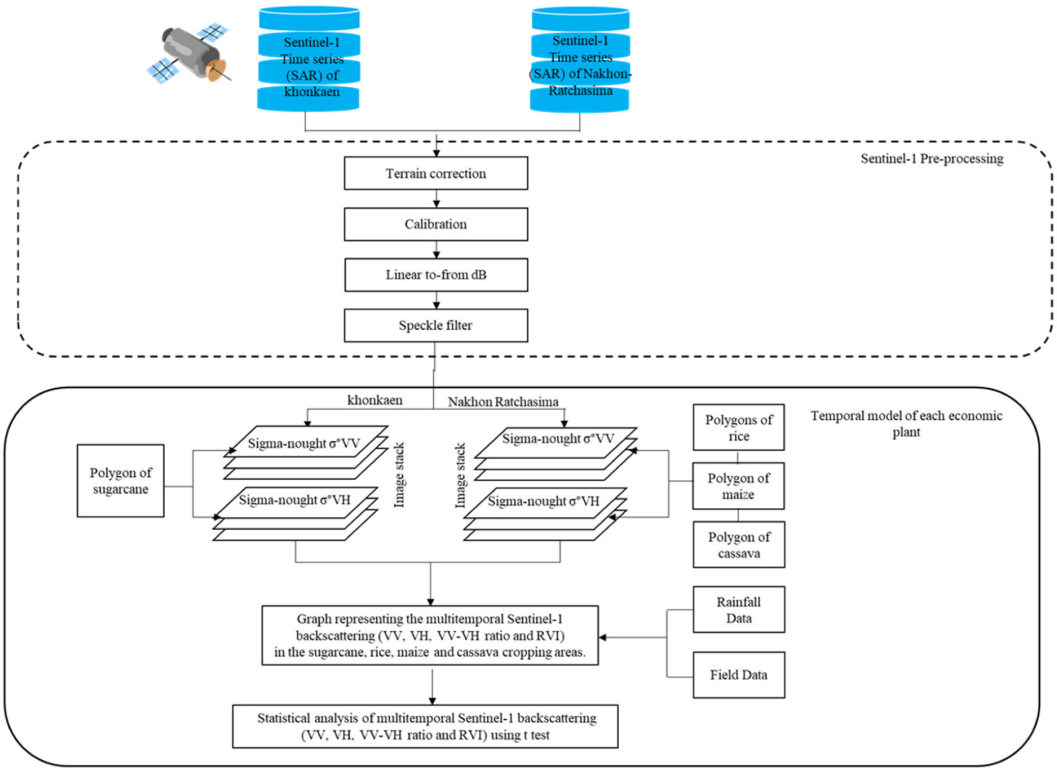

Fig. 3 Research procedures and methods

Data preparation before analysis

An initial satellite image processing step before analysis (Pre-Processing) involved adjusting the image for two main types of correction: radiometric and geometric. The steps and details of the image processing operations were: 1) adjust the terrain error (Terrain Correction) distorted from the true terrain to obtain the corrected image picture based on the Earth's surface; 2) correct radiological images (Calibration) to improve spectral reflectance, emittance or reverse scattering measurements; 3) Linear to-from dB to change the ratio of the reflected wave power to the power of the transmitted wave (backscattering) for the energy and light intensity at the time of image data collection; 4) speckle filter noise by placing a balance between reducing noise and maintaining the data structure by reducing black points on the image data using a variety of editing models, specifically a 5×5 m Lee filter with 100 plots in Nong Ruea district, Khon Kaen province (16°29′36″N, 102°26′0″E) as shown in Fig. 2A, and then creating 29 interstitial images recorded during 2019–2020 covering Nakhon Ratchasima province, while the growth of rice and cassava was monitored using 100 plots in Nakhon Ratchasima district (14°58′16″N, 102°5′59″E), as shown in Figs. 2B and 2C, respectively. In Nakhon Ratchasima province, the growth of maize was tracked in Pak Chong district (14°24′42″N, 101°25′18″E), as shown in Fig. 2D. The VV and VH polarization time series data set were extracted from satellite images in the study area by taking the difference in the backscatter between polarizations. They were generated to extract the mean backscatter and to display VV, VH, VV/VH and RVI in the graphs. The VV and VH were calculated proportionally to the positive polarization values of VV and VH, in order to the display time-series data of satellite images (Chauhan and Srivastava, 2016), as shown in Equation 2:

$$RVI=\frac{(VV-VH)}{(VV+VH)} \quad (2)$$

Satellite data with different observation times served as percentiles for the computation base by stacking them all and sorting chronologically and grouping per day. A collocated mean band from the grouped images was computed each day within the given time period. This time series product was used to create time series per pixel. Then, the correlation was analyzed between the backscatter pattern of the polarization radar signal and the level of crop growth in the field with rainfall and field data.

Statistical analysis

The mean polarization backscatter values VV, VH, VV/VH and RVI) were used to determine the time of crop cultivation based on a t test during the seeding period. The study used the two-tailed test for the four crops before and after growth. The t-critical value can be both positive and negative. The F test statistic was used to determine whether the samples were equal or not and to determine what type of t test statistic was suitable for use. For equal samples, a pooled variance t test was used, as shown in Equation 3 and for unequal samples, the t test used the separated variance as shown in Equation 4.

$$t = \frac{(X_1 - X_2)}{\sqrt{sp^2\left(\frac{1}{n_1}+\frac{1}{n_2}\right)}} \quad (3)$$

When

$$sp^2 = \frac{(n_1-1)s_1^2-(n_2-1)s_2^2}{n_1+n_2-2}$$

$$t = \frac{(X_1-X_2)}{\sqrt{\left(\frac{s_1^2}{n_1}+\frac{s_2^2}{n_2}\right)}} \quad (4)$$

where t is the test statistic (t test), $\overline{X}_2$ is the mean from sample group 1, $\overline{X}_2$ is the mean from sample group 2, s_1^2 is the variance from sample group 1, s_2^2 is the variance from sample group 2, n_1 is the amount of data from sample group 1 and n_2= is the amount of data from sample group 2.

The t test hypothesis was used to determine whether the two samples differed at a significant level ($p < 0.05$), which is a popular significance level used in research (Fisher, 1925).

Results and Discussion

Time-series data acquired from Sentinel-1 are essential and valuable for crop growth monitoring such as the crop stage and planting and harvesting dates in tropical areas because the radar signal can penetrate through cloud cover (Chen et al., 2007; Ferrant et al., 2017). However, there are some limitations with the optical sensor regarding cloud cover, making it impossible to guarantee acquisition in the monsoonal tropics. With the increased availability of time series data availability using Sentinel-1, time-series data processing methods were selected to improve the data quality by reducing spatial and temporal noise, according to Phan et al. (2018) and Phung et al. (2020). The repeat cycle of Sentinel-1 data was freely and primarily accessible in 12 d with a spatial resolution of 5 m × 20 m (range by azimuth). In addition, the availability of two satellites (Sentinel-1A and 1B) made it possible to obtain data within 6 d if available). This dataset simplified using the pixel-based approach as it was less time-consuming than the object-based approach (Hussain et al., 2013). The method identified the growth stages, based on the age determination of the rice, maize, cassava and sugarcane to facilitate a truthful assessment of the spatial distribution change among different crop cultivation regions in near real-time. Such information is important for agricultural management agencies in Thailand.

The potential of the satellite imagery to monitor crop growth status was evaluated based on the mean, differential polarization backscatter VV, VH, VV/VH ratios and RVI of crops. In total, 100 samples of each crop species were used from January 2019 to August 2020 cover cultivated rice, maize and cassava areas in Nakhon Ratchasima province and sugarcane plantations in Khon Kaen province. The results were plotted as trend graphs of correlation values, as shown in Figs. 4–15.

Rice cultivation area in Nakhon Ratchasima district, Nakhon Ratchasima province

The growth of field rice is shown in Fig. 4 in based on the 2 wk physical growth status, covering development from day 0 to the beginning of harvest at around day 120, between January 2019 to mid-August 2020. Although VH polarization is lower than for VV, the shapes of their two graphs were similar depending on soil moisture changes, with cultivation decreasing the VH, VV and RVI polarity rebound values in July. As a result of rain that had accumulated since May, there was flooding in the fields. However, this precipitation event did not influence the VV/VH polarization ratio. The backscatter sensitivity of VH, VV and RVI polarization was used to investigate changes in soil moisture. The accumulation of vegetation mass above the ground during the stem and leaf growth period (days 0–60 from 19 May 19 to 18 July 2019) resulted in the VV/VH polarization backscatter increasing after planting.

Furthermore, VH and VV polarization backscatter increased more rapidly after flooding in the field mainly due to the volume backscatter when the rice leaves unfolded. The rice crop increased during the reproductive growth period and maturing period of rice (days 61–120) from mid-July to late October. The kernels began to produce grains, resulting in a slightly higher increase in the backscatter values from VV and RVI polarization by about 0.6 dB and 0.41 dB, respectively, before

gradually decreasing and entering the maturing period. The rice crop leaves withered and the rice grains were ready to harvest in November or from day 166 and later. The VH polarization backscatter did not increase during the maturation period. This was consistent with the study of radar signals received and transmitted in different directions (cross-polarized) as this was less sensitive than radar signals received and transmitted in a similar or co-polarized field for rice cultivation areas in 2020 that were prepared for sowing in May. However, the polarization reflectance changed since March. In other plots, rice cultivation might likely begin in March.

Maize cultivation area, Pak Chong District, Nakhon Ratchasima province

Fig. 7 shows the maize growth for 2 wk in 2019, tracking the maize growth status from 7 July until harvest. VH, VV, VH/VV polarization and RVI in the unplanted areas from late March to early July changed slightly before the cultivation period due to the variability in soil moisture and cultivation preparation using various soil tilling methods, The VH polarization backscatter was lower than for VV. There were four abrupt declines in VV, VH, polarization and RVI between July and October as a result of heavy rainfall in the study area of over 30 mm and up to 80 mm, as described by Ferrer (2017) in synthetic aperture radar images. From 14 July to 30 September, the stem growth and blade periods for maize increased the stem length and created new leaves, with the rapid accumulation of above-ground biomass interspersed with rain resulting in a sudden decrease and increase in the backscatter from polarization during the last period of reproductive growth of the maize stems and leaves before they stopped growing, turning light brown.

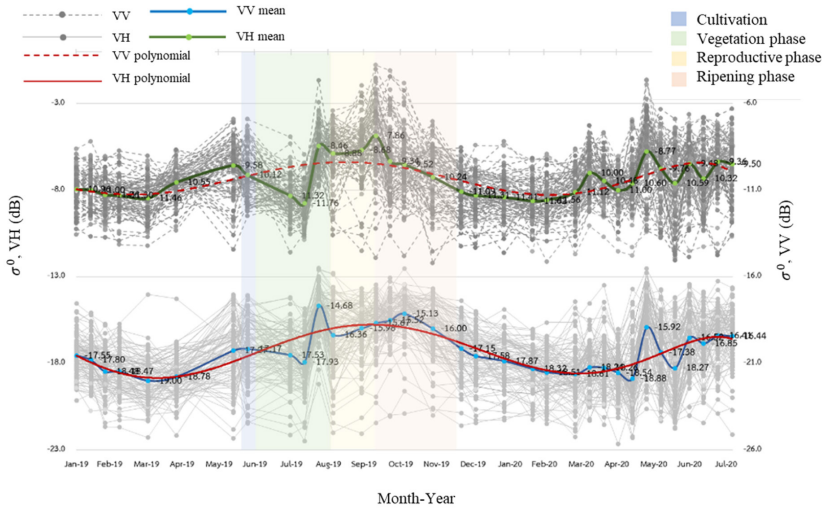

Fig. 4 Backscatter value of VH and VV (right-hand axis) polarization for rice

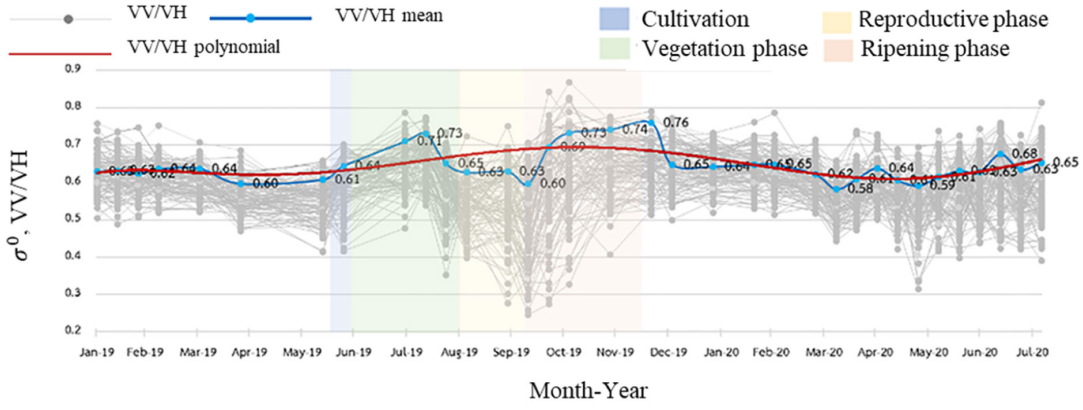

Fig. 5 VV/VH ratio polarization of rice

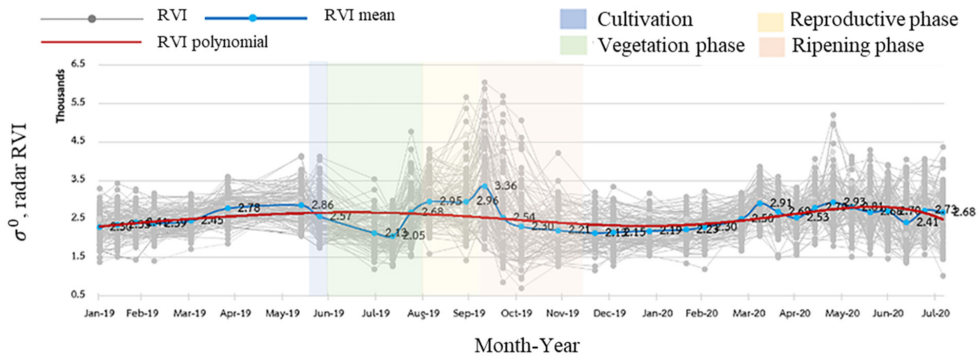

Fig. 6 Radar vegetative index (RVI) for rice

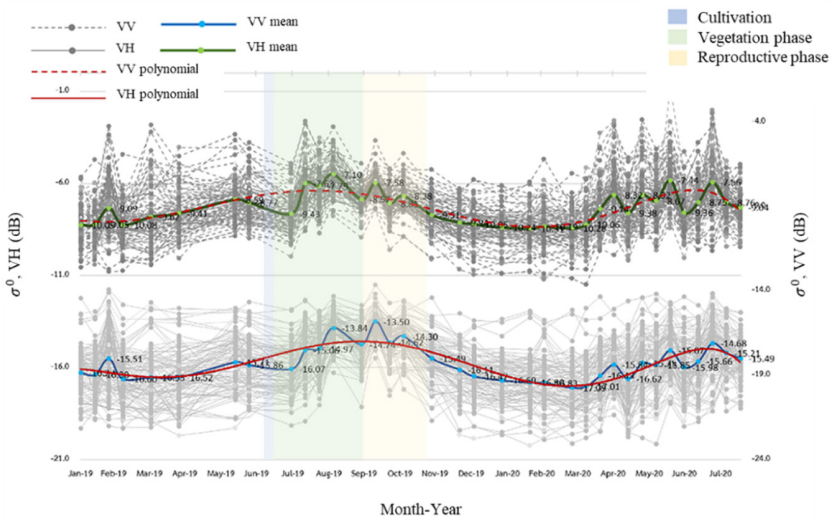

Fig. 7 Backscatter values of VH and VV (right-hand axis) polarization for maize

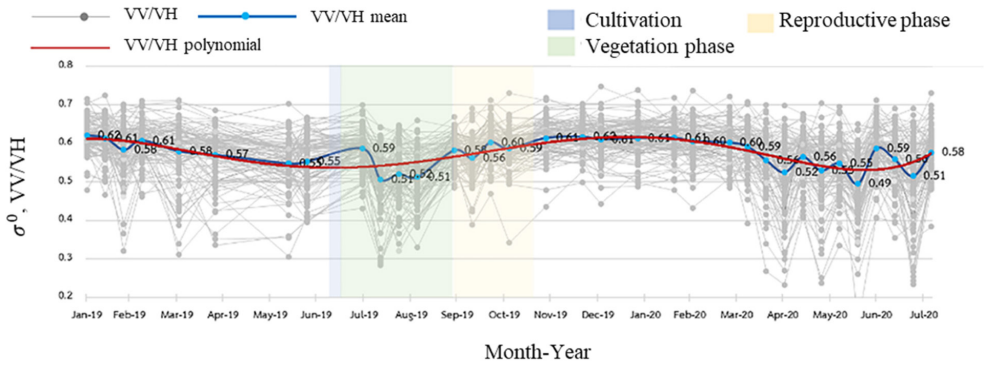

Fig. 8 VV/VH ratio polarization for maize

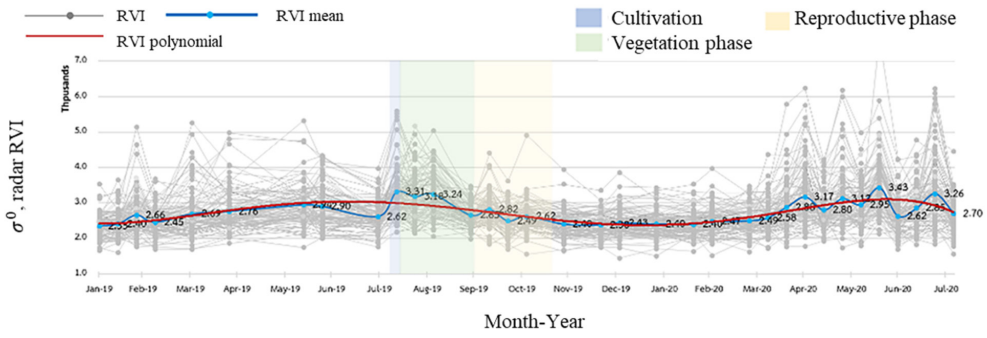

Fig. 9 Radar vegetative index (RVI) for maize

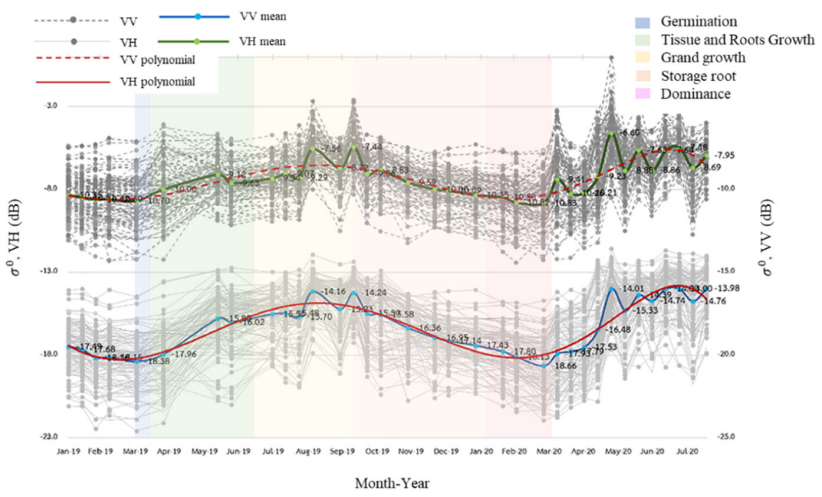

Fig. 10 Backscatter values for VH and VV (right-hand axis) polarization for cassava

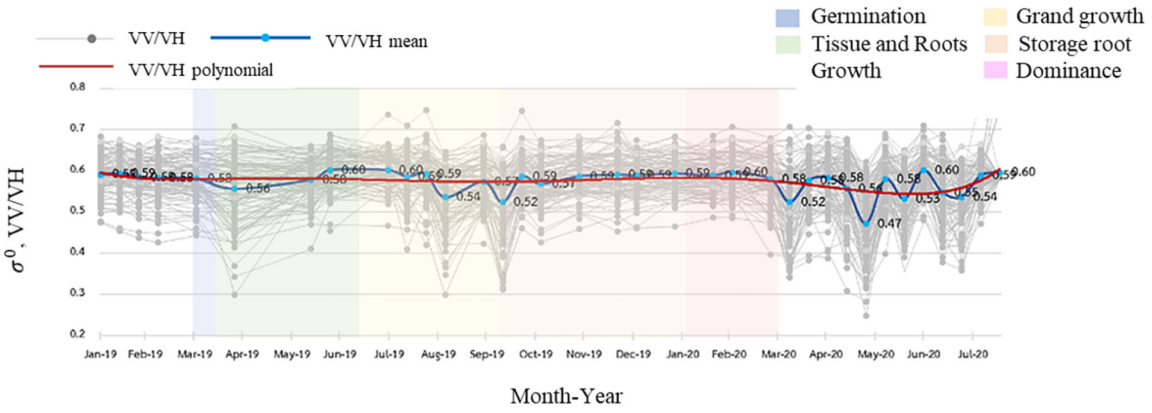

Fig. 11 VV/VH ratio polarization for cassava

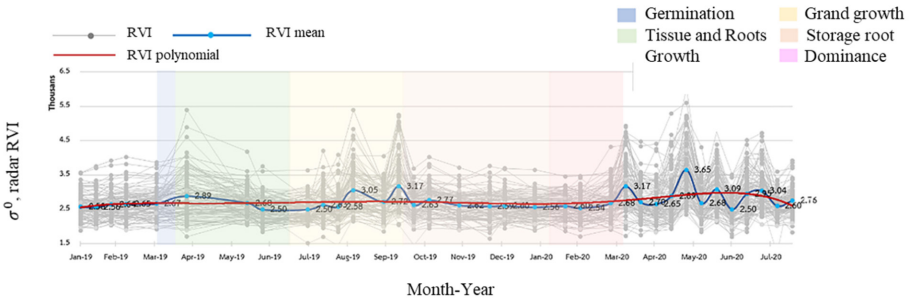

Fig. 12 Radar vegetative index (RVI) for cassava

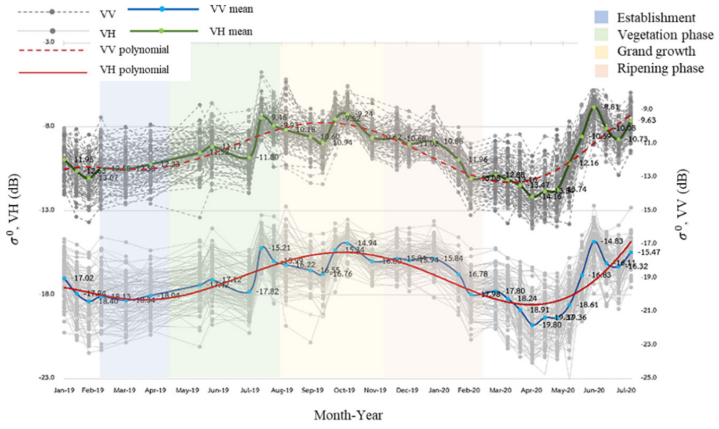

Fig. 13 Backscatter values of VH and VV polarization for sugarcane

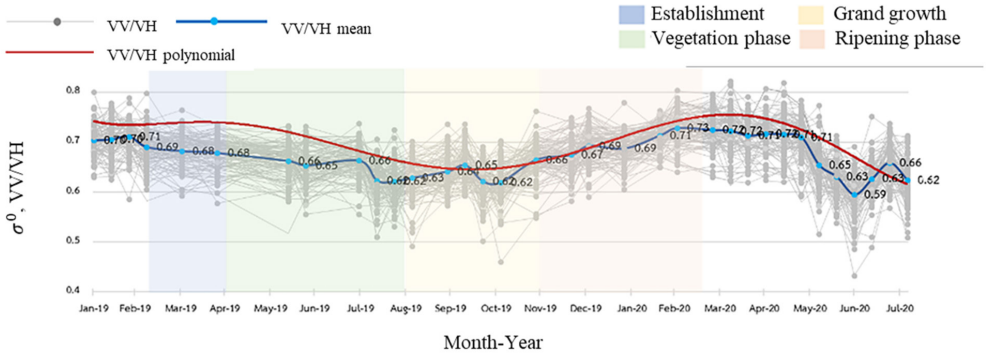

Fig. 14 VV/VH ratio polarization for sugarcane

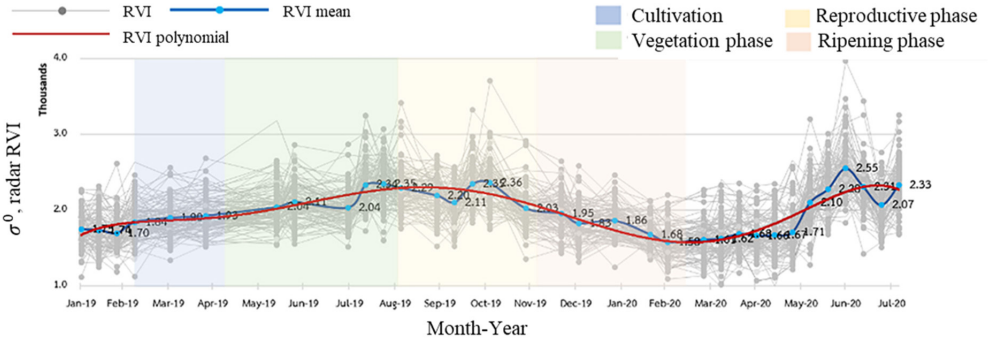

Fig. 15 Radar vegetative index (RVI) of sugarcane

The VV polarization backscatter and RVI continued to decline until harvest in late October. The VV polarization backscatter and RVI reduced to -11.41 dB and 2.15 dB, respectively, with less change than for the VH polarization during the non germination period. However, the VV/VH polarization values were not consistent with the field data and the maize growth characteristics.

Cassava cultivation area, Mueang district, Nakhon Ratchasima province

The first stage of cassava cultivation began with soil preparation involving weed tillage and tillage (Figure 10) before March. There were low rebound values from the VH polarization (-18.16 dB) and VV (-10.60 dB); then, in late March–November, the cassava produced ground cover during days 5–240. The backscatter values continued to increase to their first peak in mid-May during leaf development and root system formation, gradually decreasing at approximately day 54 as the cassava leaves withered. This was caused by the lack of water in leaf development and root formation, which corresponds to the rainfall data in July. Later the cassava grew and produced a dense canopy and near-complete soil cover with the maximum reflectance values at 2 positions were similar for VH, VV polarization and RVI. The first point was in early August, when the backscatter from the VH polarization was -14.16 dB, for VV was -7.56 dB and the RVI was 3.02 dB, while the second point was in mid-September, when the VH backscatter polarization was -14.24 dB, the VV was -7.44 dB and the 3.14 dB sudden declines in the curves were the results of rainfall greater than 40 mm in August and September. Then, the backscatter began to decline in October as the cassava leaves began to wither and fall, as the cassava entered the nutrient migration stage to the root or tuber.

Thereafter, the remaining leaves fell from the rest of the cassava. As a result, the VH and VV polarization backscatter values gradually decreased until harvest in February the following year. While the cassava leaves were wilting and falling, the RVI changed little.

Sugarcane cultivation area Khon Kaen district Khon Kaen province

Fig. 13 shows that deep tillage and grooving before sugarcane cultivation resulted in low rebound values in February (VH = -18.40 dB, VV = -13.07 dB). At days 0–60, the VH, VV polarization and RVI rose slowly, as the stems and leaf growth phases commenced. At this stage, the sugar cane started tillering. This occurred three times; the first was in July, during the growth of the stem and leaves (days 61–150), while the second and third times in September and November, respectively, were during the peak growth of the cane (days 61–180 and days 151–240).

The cane growth extended the stems and dense leaves formed, resulting in a high backscatter before decreasing after day 180. The leaves and stem began to turn brown at days 215–240, resulting in a continuous decrease in backscatter from VH, VV polarization and the RVI. However, the VV/VH polarization was not consistent with the field survey growth data and cane growth characteristics.

The statistical analysis results using the t test to compare the means of backscatter of all four crops in the same crop period and in different cultivation periods every 2 mth before and after plant growth are shown in Tables 1–4. In these tables, where the t-statistic is more significant than zero and greater than or equal to the t critical value or less than zero and less than or equal to the t-critical value, the two samples were different. Here the table results are shown with zero (0), while where the t statistic is more significant than zero and less than or equal to the t critical value, the table results are shown with a positive one (+1). Where the two samples were not different, with the t statistic less than zero and greater than or equal to the t critical value, the table results show a negative one (-1).

The results in Tables 1–4 showed that the VV, VV/VH and RVI values for the rice plots could identify the same crop range. However, during different cultivation periods, only VV/VH was able to identify the vegetation phase and ripening phase of rice. The VH, VV/VH and RVI value could specify the same crop range in different cultivation periods. At the same time, VV/VH and RVI were able to identify the vegetation phase and reproductive maturation period (Reproductive stage) of maize, cassava and sugarcane cultivation. However, no polarization value could distinguish between the different crop ranges.

Conclusion

The correlation trends for VV and VH polarization were used to monitor crop growth. The backscatter value of VV polarization was higher than for VH and it varied depending on the soil moisture, changes in the weather, soil surface, soil cover and orientation in crop cultivation. The VH, VV polarization and the RVI values changed only slightly when there was no crop cultivation. However, there was no influence on the VV/VH ratio for maize, cassava and sugarcane plantations by crop stem and leaf growth. The backscatter values from VH,

VV polarization and the RVI were significantly sensitive to canopy and stem elongation. While the crops were growing, if the backscatter of the polarization increased, there was a sudden drop as soil moisture increased or there was rain in the area during the reproductive growth of the rice and maize. This assumption was based on the SAR waves being sensitive to water or dielectric elements, so it could be suggested to use rainfall data and field surveys to assess the result. The current study investigated the usefulness of the Sentinel-1 satellite as a pioneering stage in using SAR data for agriculture in Thailand. The results indicated slightly higher VV and RVI values because of each crop cycle's maximum growth during the ripening and harvesting phases. The backscatter gradually decreased as the plant growth peak passed and the crop soil was left fallow, causing the backscatter to change slightly so the curve appeared relatively smooth. Thus, it was concluded

Table 1 Statistical t test of mean backscatter to determine rice cultivation range

Phase	Polari-zation	Month	Mean	SD	F statistic	Variance type	t statistic	Difference type
Vegetation phase	VH	Jun-19	-17.22	2.17	1.04	Pooled	1.50	0
		Jul-19	-17.53	2.25				
	VV	Jun-19	-9.85	1.15	1.06	Pooled	9.53	+1
		Jul-19	-11.32	1.22				
	VV/VH	Jun-19	0.57	0.00	1.46	Pooled	-10.77	-1
		Jul-19	0.65	0.00				
	RVI	Jun-19	2741.42	134068.44	1.20	Pooled	10.79	+1
		Jul-19	2155.19	161001.66				
Cultivation Phase - Vegetation phase	VH	Mar-19	-18.47	1.43	1.51	Separated	-6.62	-1
		Jun-19	-17.22	2.17				
	VV	Mar-19	-11.30	0.89	1.30	Pooled	-10.18	-1
		Jun-19	-9.85	1.15				
	VV/VH	Mar-19	0.61	0.00	1.19	Pooled	6.69	+1
		Jun-19	0.57	0.00				
	RVI	Mar-19	2411.03	98160.27	1.37	Pooled	-6.86	-1
		Jun-19	2741.42	134068.44				
Vegetation phase - Ripening Phase	VH	Jun-19	-17.22	2.17	1.62	Separated	-8.66	-1
		Oct-19	-15.60	1.34				
	VV	Jun-19	-9.85	1.15	2.83	Separated	-5.94	-1
		Oct-19	-8.60	3.27				
	VV/VH	Jun-19	0.57	0.00	5.75	Separated	1.75	0
		Oct-19	0.55	0.01				
	RVI	Jun-19	2741.42	134068.44	6.53	Separated	-2.36	-1
		Oct-19	2978.50	875711.12				

Table 2 Statistical t test of mean backscatter to determine maize cultivation range

Phase	Polari-zation	Month	Mean	SD	F statistic	Variance type	t statistic	Difference type
Vegetation phase	VH	Aug-19	-15.02	1.28	2.27	Separated	-5.35	-1
		Sep-19	-14.29	0.57				
	VV	Aug-19	-7.71	1.10	2.09	Separated	0.97	0
		Sep-19	-7.83	0.53				
	VV/VH	Aug-19	0.51	0.00	2.10	Separated	-4.30	-1
		Sep-19	0.55	0.00				
	RVI	Aug-19	3242.29	337754.95	2.31	Separated	4.25	+1
		Sep-19	2946.55	146231.87				
Vegetation phase _ Reproductive phase	VH	Jun-19	-15.79	1.81	3.21	Separated	-9.71	-1
		Sep-19	-14.29	0.57				
	VV	Jun-19	-8.68	1.17	2.22	Separated	-6.50	-1
		Sep-19	-7.83	0.53				
	VV/VH	Jun-19	0.55	0.00	1.82	Separated	0.43	0
		Sep-19	0.55	0.00				
	RVI	Jun-19	2921.77	268011.32	1.83	Separated	-0.38	0
		Sep-19	2946.55	146231.87				
Vegetation phase _ Reproductive phase	VH	Sep-19	-14.29	0.57	2.52	Separated	4.10	+1
		Oct-19	-14.87	1.42				
	VV	Sep-19	-7.83	0.53	1.21	Pooled	3.67	+1
		Oct-19	-8.19	0.43				
	VV/VH	Sep-19	0.55	0.00	1.20	Pooled	-5.83	-1
		Oct-19	0.58	0.00				
	RVI	Sep-19	2946.55	146231.87	1.35	Pooled	5.81	+1
		Oct-19	2652.98	108667.33				

Table 3 Statistical t test of mean backscatter to determine cassava cultivation range

Phase	Polari-zation	Month	Mean	SD	F-statistic	Variance type	t-statistic	Difference type
Main growth phase	VH	Jul-19	-15.53	1.72	1.10	Pooled	0.32	0
		Aug-19	-15.59	1.89				
	VV	Jul-19	-9.34	1.07	1.07	Pooled	-1.10	0
		Aug-19	-9.18	1.15				
	VV/VH	Jul-19	0.60	0.00	1.40	Pooled	2.00	+1
		Aug-19	0.59	0.00				
	RVI	Jul-19	2497.50	99786.51	1.49	Pooled	-2.08	-1
		Aug-19	2601.00	148703.08				
Tissue and roots growth phase – Main growth	VH	Apr-19	-18.17	2.31	1.22	Pooled	-12.58	-1
		Aug-19	-15.59	1.89				
	VV	Apr-19	-10.35	2.32	2.02	Separated	-6.29	-1
		Aug-19	-9.18	1.15				
	VV/VH	Apr-19	0.57	0.00	1.57	Separated	-2.69	-1
		Aug-19	0.59	0.00				
	RVI	Apr-19	2776.17	251874.62	1.69	Separated	2.77	+1
		Aug-19	2601.00	148703.08				
Main growth - Dominance phase	VH	Aug-19	-15.59	1.89	1.33	Pooled	-3.98	-1
		Feb-20	-14.87	1.42				
	VV	Aug-19	-9.18	1.15	1.28	Pooled	-6.53	-1
		Feb-20	-8.25	0.89				
	VV/VH	Aug-19	0.59	0.00	1.48	Pooled	4.62	+1
		Feb-20	0.55	0.00				
	RVI	Aug-19	2601.00	148703.08	2.29	Separated	-4.06	-1
		Feb-20	2884.62	340245.43				

Table 4 Statistical t test of mean backscatter to determine sugarcane cultivation range

Phase	Polari-zation	Month	Mean	SD	F statistic	Variance type	t statistic	Difference type
Establishment phase	VH	Mar-19	-17.27	0.96	1.89	Separated	5.16	+1
		Apr-19	-18.13	1.81				
	VV	Mar-19	-12.50	1.32	1.34	Pooled	-0.90	0
		Apr-19	-12.36	0.98				
	VV/VH	Mar-19	0.69	0.00	70.45	Separated	0.34	0
		Apr-19	0.68	0.09				
	RVI	Mar-19	1843.17	60645.51	1.36	Pooled	-2.18	-1
		Apr-19	1913.97	44744.17				
Establishment phase – Main growth	VH	Apr-19	-18.13	1.81	3.97	Separated	-13.75	-1
		Oct-19	-16.05	0.46				
	VV	Apr-19	-12.36	0.98	2.53	Separated	-18.21	-1
		Oct-19	-10.23	0.39				
	VV/VH	Apr-19	0.68	0.00	1.36	Pooled	11.03	+1
		Oct-19	0.64	0.00				
	RVI	Apr-19	1913.97	44744.17	1.24	Pooled	-11.01	-1
		Oct-19	2227.08	36118.43				
Main growth – Ripening phase	VH	Oct-19	-16.05	0.46	2.79	Separated	19.15	+1
		Apr-20	-18.58	1.28				
	VV	Oct-19	-10.23	0.39	2.73	Separated	26.25	+1
		Apr-20	-13.39	1.06				
	VV/VH	Oct-19	0.64	0.00	1.88	Separated	-18.80	-1
		Apr-20	0.72	0.00				
	RVI	Oct-19	2227.08	36118.43	1.57	Separated	18.84	+1
		Apr-20	1653.31	56647.68				

that VV, VH polarization and RVI values could be used to track crop growth from planting to harvest. However, when the leaves began to wilt or turned light brown, there was little or no influence on the RVI. The VV/VH ratio was sensitive to rice growth after cultivation based on analysis using the t test technique to compare the means of backscatter of all four crops during the same crop period and between two different crop periods. It was concluded that rice (VV polarization, VV/VH and RVI), maize (VH polarization, VV/VH and RVI), cassava (VV and VH polarization), and sugarcane (VH polarization and RVI) could be used to specify the same crop range.

In contrast, VV/VH polarization of rice and using VV/VH and the RVI for maize could be used to identify different crop ranges. No polarization type was able to specify cassava or sugarcane for different cultivation ranges. Finally, a limitation of the study was that the period of data collection was unusual

as it covered the drought in Thailand in 2019, so the effect on the research result may have been slightly different from normal conditions. Nonetheless, this case could be used as a baseline for further research investigating other periods of either average or severe weather.

Conflict of Interest

The authors declare that there are no conflicts of interest.

Acknowledgements

This work was prepared under the cassava crop monitoring project, which received research grants from the Kasetsart University Research and Development Institute (KURDI), Bangkok, Thailand. The ASF DAAC 2019–2020 containing modified Copernicus Sentinel data 2019–2020 was processed by ESA. Ms Chitayaporn Srithasri, aided with proof reading of the radar signal characteristic for crop monitoring in Thailand.

References

Agromax Micronutrients Pvt. Ltd. 2018. Growth Stages of Corn. Maharashtra, India. https://medium.com/@brandevergreen1991/growth-stages-of-corn-289d26846e43, 15 May 2020.

Aguilar, A. 2019. Machine learning and big data techniques for satellite-based rice phenology monitoring. Doctoral dissertation, University of Manchester. Manchester, UK.

Aschbacher, J., Milagro-Pérez., M.P. 2012. The European Earth monitoring (GMES) programme: Status and perspectives. Remote Sens. Environ. 120: 3–8. doi.org/10.1016/j.rse.2011.08.028

Baghdadi, N., Todoroff, P., Zribi, M. 2011. Multitemporal observations of sugarcane by TerraSAR-X sensor. In: The 2011 IEEE International Geoscience and Remote Sensing Symposium. Vancouver, BC, Canada, pp. 1401-1404.

Chauhan, S., Srivastava, H.S. 2016. Comparative evaluation of the sensitivity of Multi-polarized SAR and optical data for various land cover classes. Int. J. Remote Sens. 4: 1–14.

Chen, J., Lin, H., Pei, Z. 2007. Application of ENVISAT ASAR data in mapping rice crop growth in Southern China. IEEE Geosci. Remote S. 4: 431–435. doi: 10.1109/LGRS.2007.896996

Earth-i's Techniques. 2019. RADAR vs OPTICAL Earth Observation – Why both? Surrey, United Kingdom. https://earthi.space/blog/radar-vs-optical-earth-observation-why-both/, 26 May 2020.

Ferrant, S., Selles, A., Le Page, M., et al. 2017. Detection of irrigated crops from Sentinel-1 and Sentinel-2 data to estimate seasonal groundwater use in South India. Remote Sens. 9: 1–21. doi.org/10.3390/rs9111119

Ferrer, V. 2017. SAR images show water in a dark tone. Is it due to reflection or absorption? Kerala, India. https://www.researchgate.net/post/SAR_images_show_water_in_dark_tone_Is_it_due_to_reflection_or_absorption#:~:text=Generally%20in%20Synthetic%20Aperture%20Radar,the%20radar%20(specular%20reflection), 10 June 2020.

Fisher, R.A. 1925. Applications of Student's distribution. Metron 5: 90–194.

Hussain, M., Chen, D., Cheng, A., Wei, H., Stanley, D. 2013. Change detection from remotely sensed images: From pixel-based to object-based approaches. ISPRS J. Photogramm. 80: 91–106. doi: 10.1016/j.isprsjprs.2013.03.006.

Mattia, F., Toan, T.L., Picard, G., et al. 2003. Multitemporal C-band radar measurements on wheat fields. IEEE T. Geosci. Remote 41: 1551–1560. doi: 10.1109/TGRS.2003.813531

Minh, H.V.T., Avtar, R., Mohan, G., Misra, P., Kurasaki, M. 2019. Monitoring and mapping rice cropping pattern in flooding area in the Vietnamese Mekong Delta using Sentinel-1A data: A case of Giang Province. ISPRS Int. J. Geo-Inf. 8: 211. doi.org/10.3390/ijgi8050211

Nakhon Ratchasima province. 2020. General information of province. Nakhon Ratchasima, Thailand. https://www2.nakhonratchasima.go.th/content/general, 10 June 2020. [in Thai]

Office of the Cane and Sugar Board. 2019. Report on sugarcane planting areas in the production year 2018/19. Bangkok, Thailand. http://www.ocsb.go.th/upload/journal/fileupload/923-9040.pdf, 15 June 2020. [in Thai]

Phan, H., Le Toan, T., Bouvet, A., Nguyen, L.D., Pham Duy, T., Zribi, M. 2018. Mapping of rice varieties and sowing date using X-band SAR data. Sensors 18: 316. doi.org/10.3390/s18010316

Phung, H.P., Nguyen, L.D., Nguyen-Huy, T., Le-Toan, T., Apan, A.A. 2020. Monitoring rice growth status in the Mekong Delta, Vietnam using multitemporal Sentinel-1 data. J. Appl. Remote Sens. 14: 014518. doi.org/10.1117/1.JRS.14.014518.

Satalino, G., Balenzano, A., Mattia, F., Davidson, M.W. 2013. C-band SAR data for mapping crops dominated by surface or volume scattering. IEEE Geosci. Remote S. 11: 384–388.

Schmitt, A., Brisco, B. 2013. Wetland monitoring using the curvelet-based change detection method on polarimetric SAR imagery. Water 5: 1036–1051. doi.org/10.3390/w5031036

Srikanth, P., Chakraborty, A., Murthy, C.S. 2021. Crop monitoring using microwave remote sensing. In: Mitran, T., Meena, R.S., Chakraborty, A. (Eds.). Geospatial Technologies for Crops and Soils. Springer. Singapore, pp. 201–228. https://doi.org/10.1007/978-981-15-6864-0_5

The European Space Agency. 2020. Sentinel-1 SAR User Guide Introduction. Paris, France. https://sentinel.esa.int/web/sentinel/user-guides/sentinel-1-sar, 18 April 2020.

Organization for Economic Cooperation and Development. 2016. Cassava (*Manihot esculenta*). In: OECD Working Group on the Harmonisation of Regulatory

Oversight in Biotechnology (Ed.). Safety Assessment of Transgenic Organisms in the Environment, Vol. 6. OECD Publishing. Paris, France, pp. 155–186. doi.org/10.1787/9789264253421-en

Veloso, A., Mermoz, S., Bouvet, A., Toan, T.L., Planells, M., Dejoux, J.F., Ceschia, E. 2017. Understanding the temporal behaviour of crops using Sentinel-1 and Sentinel-2-like data for agricultural applications. Remote Sens. Environ. 199: 415–426.